International Journal of Science and Research (IJSR)
ISSN: 2319-7064
SJIF (2022): 7.942

Analysis and Design Optimization of Hallow Section Valve Springs

Jagadish. R. Bagali[1], R. S. Matti[2], B. S. Vivekanand[3]

[1]Basaveshwar Engineering College, Vidyagiri, Bagalkote, Karnataka, India-567102
Email: *jagadish.r.bagali[at]gmail.com*

[2]Professor, Basaveshwar Engineering College, Vidyagiri, Bagalkote, Karnataka, India-567102
Email: *rajumattikpl[at]gmail.com*

[3] Professor, Basaveshwar Engineering College, Vidyagiri, Bagalkote, Karnataka, India-567102
Email: *vivekanand.bs[at]gmail.com*

Abstract: ***Valve spring is designed for fatigue life and the natural frequency of the valve spring is an important performance measure apart from the stress and deflection [7,8,9]. The natural frequency of the valve spring should be as high as possible to avoid spring resonance at higher engine speeds and consequently the valve floating. In this work a hallow section spring with free length 59 mm, mean diameter 33.58 mm and outer wire diameter of 5 mm is considered [9]. The pitch and the inner diameter are varied to study the effect on the stress induced, deflection and natural frequencies of the spring [1]. The material considered for the analysis is chrome vanadium steel. The analytical equations are modified to include hallow section and the effect of helix angle [2]. The spread sheet program is used to determine different stresses, deflection, and natural frequency for different dimensions of the spring. The spread sheet program is also used for the purpose of selecting optimized springs among the sample data generated. The analytical results are validated using Ansys 2022R1. The bore ratio vs natural frequency curve has the highest slope and hence natural frequency change is highest with unit change in bore ratio.***

Keywords: Hallow helical springs, valve springs, fatigue life, natural frequency, spring optimization

1. Introduction

Springs are flexible mechanical components used in many mechanical systems for positioning of components, shock absorption, energy storing devices and measurement devices [10].

These springs are classified based on the type of wire section and type of coil. The springs based on type wire section are round solid section, hallow round section, elliptical section, hallow elliptical section, and ovate section springs [8].

The stress induced in the round section spring is higher at the inside surface of the wire than the outer wire surface. This stress is zero at the center. The stress at both the surface are also opposite to each other [10, 11, 14].

The materials used for manufacturing of the springs are Stainless steel (ASTM 313), phosphor bronze steel (ASTM 314), plain carbon oil-tempered steel (ASTM 229), plain carbon hard drawn steel wire (ASTM 227), chrome vanadium steel (ASTM 231), chrome silicon steel (A401), and music wire (ASTM 228). The low wire diameter springs are cold drawn and big wire diameters springs are hot drawn [10, 12].

The springs can be used under low cycle or high cyclic loading conditions. The springs for low cyclic or static loading conditions are designed using shear stress or strain energy failure theories. The springs for high cyclic loading conditions are designed considering fatigue life and hence fatigue failure theories such as “Gerber failure theory” “Goodman failure theory” or “Soderberg failure theory” are used [10, 14].

The natural frequency of the springs depends on the stiffness of the spring and weight of the spring. the natural frequency must be at least 13 times higher than the excitation frequency to avoid the surging of the spring. surging of the spring leads to higher amplitude deformations and hence higher stress. Hence surging may lead to early failure of the springs [10].

The stress induced and deflections also depend on the pitch of the spring. The common analytical equations do not consider the effect of helix angle. The effect of helix angle for low pitch springs is negligible but for springs with higher pitch, the bending stress due to helix angle cannot be neglected [2, 10, 13].

2. Literature Survey

Mohanad Hamed Mosa et al., (2020) [1] In this investigation, FEM software is used to study the hallow cross section springs of four different bore ratios under static loading conditions. AISI 347 annealed stainless steel was used. The investigators concluded that reducing the spring's mass had no influence on shear stress, deflection, and stiffness.

Bert, C. W., (1959) [2] In this study, the equations of induced shear stress and deflection for hollow section helical springs were derived while taking the influence of helix angle into consideration. Additionally, the results and experimental results were very well matched. At the conclusion of this paper, it is noted that hollow cross section springs have a modest advantage over solid springs in terms of shear stress and deflection due to their less weight.

Pawar & Desale., (2018)[3]In this study, the author adjusted the three-wheeler spring already in use and changed the turn numbers to investigate the impact on spring properties including induced shear stress, deflection, and stiffness. IS 4454 was the material chosen. To determine the relationship between load and deflection, static structural analysis is performed. The stiffness of the spring is measured through an experiment. A 10% length decrease, 10% weight reduction, and 7% change in stiffness were shown to be feasible.

Sagar Singh Kushwaha et al., (2021) [4] In this study, springs made of four different materials were subjected to analytical and numerical analysis using Ansys software to determine spring performance characteristics like deflection and shear stress. The result was that, when greater deflection was considered, the spring material ASTM 228 had better qualities than the previous material ASTM 227.

Liu.H&Kim.D., (2009) [5]The author suggests a method for figuring out the natural frequencies of different kinds of valve springs, such as constant pitch springs, progressive springs, etc. Additionally, he clarifies why experimental or finite element approaches and analytical formulae provide different estimates of natural frequency. The impact of end coils is not considered in the mathematical formulae. By considering the end coil effects, the author suggests a new technique for determining the natural frequency of the valve springs. The inaccuracy in the natural frequency estimation between the analytical equations and the experimental or finite element approach is significantly decreased once this error is accounted for in the analytical equations.

Taktak et al., (2014) [6] In this study, an optimization algorithm-based numerical technique is created. The optimization algorithm's inputs are spring physical characteristics such as coil clash, induced shear stress, deflection, fatigue strength, and natural frequency. MATLAB software is used to simulate the numerical model. In addition, four MATLAB optimization functions are used for the optimization process.

Hong Yan Li et al., (2011) [7] In this paper, the stress distribution in the valve spring is determined from engine speed 1000 rpm to 5000 rpm. The solid works software is used to create the CAD model and then imported into the Ansys software. The displacements are applied to the spring's upper turn, which has a fixed bottom turn. Up to 1000 rpm, the stress distribution is normal. The stress distribution is erratic at 5000 rpm. When the valve is fully open, the stress is at its highest, and when it is closed, it is at its lowest. The computed fatigue safety factor, which ranges from 1.3 to 1.7, is 1.335. There is also a discussion on the construction of valve springs and the impact of the valve mechanism's flexibility on high-speed operations.

3. Problem Definition

The objective of this work is to generate equations for hallow section springs considering the effect of helix angle by modifying the standard equations. Determination of impact of variation of pitch and inner diameter of hallow section spring on induced stresses, deflection, and natural frequency. Establishing an automated process of selection of suitable spring dimensions considering fatigue stress levels, deflection, and natural frequency.

4. Materials and Methodology

4.1. Analytical Method

The material used for the spring for this study is chrome vanadium steel with fallowing properties.

Table 1: Chrome vanadium spring mechanical properties [4, 12].

Sl. No	Material Name	Density kg/m3	Elastic Modulus MPa	Fatigue Strength MPa	Poisson Ratio	Shear Modulus MPa	Ultimate Tensile Strength MPa	Tensile Yield Strength MPa
1	Chrome Vanadium ASTM 231	7800	190000	1000	0.29	77200	1790	1570

The fallowing spring physical dimensions are used for the analysis.

Table 2: Physical spring dimensions used for the analysis [15]

Free length, L_f mm	Coil diameter, D mm	Outer wire diameter, d_o mm	Inner diameter, d_i mm	Number of turns
59	28.58 to 33.58	5	0 to 2.5	2 to 6

The initial load on the inlet valve spring to keep the inlet valve properly closed is 392 N.

The valve lift considered for proper breathing of the engine is 10 mm. The cam load considered on the valve spring, when the valve is fully open is 760.84 N to generate a lift of 10 mm.

Determination of tubular spring pitch [11]

$$For\ springs\ with\ plain\ ends, the\ pitch, p = \frac{(L_f - d_o)}{n_a} = \frac{(59-5)}{5} = \mathbf{10.8\ mm} \quad \ldots\ldots\ldots \quad (1)$$

Determination of tubular spring Helix angle [13]

$$Helix\ angle, \alpha = atan\left(\frac{p}{\pi D}\right), \alpha = atan\left(\frac{10.8}{3.14 \times 33.58}\right) = \mathbf{5.84\ degree} \quad \ldots\ldots\ldots \quad (2)$$

Determination of weight of the spring considering the helix angle [13]

Weight of spring = length of spring wire × sectional area of wire × density

$$Weight\ of\ spring = \frac{n_a \pi D}{cos\alpha} \times \frac{\pi(d_o^2 - d_i^2)}{4} \times \rho \quad kg \qquad \ldots\ldots\ldots \quad (3)$$

$$= \frac{5 \times 3.14 \times 33.58 \times 3.14 \times (5^2 - 2.5^2) \times 7.8 \times 10^{-6}}{\cos(5.84) \times 4}$$

$$= \mathbf{0.0609\ kg}.$$

Determination of tubular spring Bore ratio [2]

$$The\ bore\ ratio, B = \frac{Inner\ wire\ diameter}{Outer\ wire\ diameter} = \frac{5}{2.5} = \mathbf{0.5} \qquad \ldots\ldots\ldots \quad (4)$$

Determination of Spring Index [2, 10, 12, 13]

$$spring\ Index, C = \frac{Coil\ Mean\ Diameter}{Wire\ diameter} = \frac{33.58}{5} = \mathbf{6.716} \qquad \ldots\ldots\ldots \quad (5)$$

Determination of tangent of helix angle

$$\alpha' = \tan(\alpha) = \tan(5.845) = \mathbf{0.1023} \qquad \ldots\ldots\ldots \quad (6)$$

Determination of correction factor for spring deflection [2]

$$\psi_p = 1 - \frac{3}{16C^2} + \frac{3B^2}{8C^2} + \frac{3+\nu}{2(1+\nu)}\alpha'^2 \qquad \ldots\ldots\ldots \quad (7)$$

$$\psi_p = 1 - \frac{3}{16 \times 6.716^2} + \frac{3 \times 0.5^2}{8 \times 6.716^2} + \frac{3 + 0.29}{2(1 + 0.29)} \times 0.1023^2 = \mathbf{1.0112}$$

Determination of contraction for minimum load (392N), when valve is closed, using modified analytical equation considering the effect of helix angle [2, 9, 10].

$$y_i = \frac{8\psi_p W D^3 (n_a - 1)}{G(d_o^4 - d_i^4)} \qquad \ldots\ldots\ldots \quad (8)$$

$$= \frac{8 \times 1.0112 \times 392 \times 33.58^3 \times (5-1)}{77200(5^4 - 2.5^4)} = \mathbf{10.6\ mm}$$

$$stiffness\ of\ spring, K = \frac{W}{y_i} = \frac{392}{10.6} = \mathbf{36.9\ \frac{N}{mm}} \qquad \ldots\ldots\ldots \quad (9)$$

Determination of contraction for maximum load for 10 mm valve lift when the valve is opened, using analytical equation considering the effect of helix angle [2, 8, 9, 10].

$$Stiffness\ of\ Load\ for\ maximum\ contraction = K \times (y_i + 10) \qquad \ldots\ldots\ldots \quad (10)$$

$$= 36.9 \times (10.6 + 10) = \mathbf{760.84\ N}$$

The analytical relation for highest stress due to shear of tube section spring considering helix angle effect is as below.

$$\tau_{mx} = \frac{8WDd_o cos\alpha}{\pi(d_o^4 - d_i^4)}\left(1 + \frac{5}{4C} + \frac{7}{8C^2} + \frac{1}{C^3}\right) \qquad \ldots\ldots\ldots \quad (11)$$

$$\tau_{mx} = \frac{8 \times 760.84 \times 33.58 \times 5 \times \cos(5.84)}{3.14 \times (5^4 - 2.5^4)}\left(1 + \frac{5}{4 \times 6.716} + \frac{7}{8 \times 6.716^2} + \frac{1}{6.716^3}\right)$$

$$= \mathbf{667.63\ MPa}$$

Similarly, the minimum Shear stress of tube section spring considering helix angle effect.

$$\boldsymbol{\tau_{mn}} = \frac{8 \times 392 \times 33.58 \times 5 \times \cos(5.84)}{3.14 \times (5^4 - 2.5^4)}\left(1 + \frac{5}{4 \times 6.716} + \frac{7}{4 \times 6.716^2} + \frac{1}{6.716^3}\right)$$

$$= \mathbf{343.7\ MPa}$$

The equation for determining stress due to bending induced into the tubular spring wire due to helix angle is as below [10].

$$\sigma_{bmx} = \frac{16WDd_o sin\alpha}{\pi(d_o^4 - d_i^4)}\left(1 + \frac{1.12}{C} + \frac{0.64}{C^2}\right) \qquad \ldots\ldots\ldots \quad (12)$$

$$\sigma_{bmx} = \frac{16 \times 760.84 \times 33.58 \times 5 \times \sin(5.845)}{3.14 \times (5^4 - 2.5^4)}\left(1 + \frac{1.12}{6.716} + \frac{0.64}{6.716^2}\right) = \mathbf{133.54\ MPa}$$

$$\sigma_{bmn} = \frac{16 \times 392 \times 33.58 \times 5 \times \sin(5.845)}{3.14 \times (5^4 - 2.5^4)}\left(1 + \frac{1.12}{6.716} + \frac{0.64}{6.716^2}\right) = \mathbf{68.7\ MPa}$$

The maximum and minimum equivalent shear stress are determined using Von Mises strain energy theory [10].

$$\tau_{emx} = \tau_{mx}\sqrt{1+\frac{\sigma_{bmx}^2}{3\tau_{mx}^2}} \quad \ldots\ldots\ldots\ldots (13)$$

$$\tau_{emx} = 667.67\sqrt{1+\frac{133.54^2}{3\times 667.63^2}} = \mathbf{672.06\ MPa}$$

$$similarly, \tau_{emn} = \tau_{mn}\sqrt{1+\frac{\sigma_{bmn}^2}{3\tau_{mn}^2}}$$

$$\tau_{emn} = 343.7\sqrt{1+\frac{68.7^2}{3\times 343.7^2}} = \mathbf{345.9\ MPa}$$

The principal stresses for maximum spring load are determined as below [10].

$$\sigma_{mx\,1,2} = \frac{\sigma_{bmx}}{2} \pm \sqrt{\tau_{mx}^2 + \frac{\sigma_{bmx}^2}{4}} \quad \ldots\ldots\ldots\ldots (14)$$

$$\boldsymbol{\sigma_{mx1,2}} = \frac{133.54}{2} \pm \sqrt{667.63^2 + \frac{133.54^2}{4}} == \mathbf{737.73\ MPa, -604.18\ MPa}$$

The Von-Mises stress is determined for maximum load is as below [11]

$$\sigma_{vms} = \sqrt{\sigma_1^2 + \sigma_2^2 - \sigma_1 \times \sigma_2} \quad \ldots (15)$$

$$\sigma_{vms} = \sqrt{737.7^2 + (-604.18)^2 + 737.7 \times 604.18}$$

$$= \mathbf{1164.05\ MPa}$$

The rotational natural vibration rate of tubular spring can be determined as below.

$$\omega_n = \frac{1}{2\sqrt{2}\ \times \pi D^2(n_a - 2.5)}\sqrt{\frac{1000G(d_o^4 - d_i^4)cos\alpha}{\rho\psi_p(d_o^2 - d_i^2)}} \quad \ldots\ldots\ldots\ldots (16)$$

$$= \frac{1}{2\sqrt{2}\ \times 3.14 \times 33.58^2(5-2.5)}\sqrt{\frac{1000 \times 77200(5^4 - 2.5^4)cos(5.845)}{7.8\times 10^{-6} \times 1.011(5^2 - 2.5^2)}}$$

$$\mathbf{696.3\ rps}$$

Determination of fatigue factor of safety [6,11]

Torsional rupture modulus for spring material is determined as below [11].

$$\tau_{su} = 0.67\sigma_{UTS} = 0.67 \times 1790 = \mathbf{1199.3 MPa} \quad \ldots\ldots\ldots\ldots (17)$$

Torsional yield strength for spring material is calculated as below. [11].

$$\tau_{ys} = 0.56\sigma_{UTS} = 0.56 \times 1790 = \mathbf{1002.4 MPa} \quad \ldots\ldots\ldots\ldots (18)$$

Determine endurance limit using Zimmerli data and equation considering the spring as shot peened, and Soderberg failure theory [11].

$$\tau_{es} = \frac{\tau_{za}}{1 - \left(\frac{\tau_{zm}}{\tau_{ys}}\right)} \quad \ldots\ldots (19)$$

$$\boldsymbol{here},$$

$$\tau_{za} = 398\ MPa, Torsional amplitude stress as per Zimmerli data [11]$$

$$\tau_{zm} = 534\ MPa, Torsional mean stress as per Zimmerli data\ [11]$$

$$\tau_{es} = \frac{398}{1 - \left(\frac{534}{1002.4}\right)} = \mathbf{851.7 MPa}$$

To determine the fatigue safety factor, the mean and amplitude shear stress values are required. [11].

$$Mean\ equivalent\ shear\ stress, \tau_{em} = \frac{(\tau_{emx} + \tau_{emn})}{2} \quad \ldots\ldots\ldots (20)$$

$$\tau_{em} = \frac{(672.06 + 345.9)}{2} = \mathbf{509.03 MPa}$$

$$Amplitude\ equivalent\ shear\ stress, \tau_{ea} = \frac{(\tau_{emx} - \tau_{emn})}{2} \quad \ldots\ldots (21)$$

$$\tau_{ea} = \frac{(672.06 - 345.9)}{2} = \mathbf{163.03\ MPa}$$

Fatigue factor of safety considering Soderberg failure theory is as below [11]

$$\left(\frac{\tau_{ea}}{\tau_{es}}+\frac{\tau_{em}}{\tau_{ys}}\right)^{-1}=FOS_s \qquad \ldots\ldots\ldots \qquad (22)$$

$$\left(\frac{163.03}{851.7}+\frac{509.03}{1002.4}\right)^{-1}=FOS_s=\mathbf{1.43}$$

Since the recommended fatigue factor of safety for helical springs ranges from 1.3 to 1.7, the above spring with its physical dimensions and material under given minimum and maximum load has 10 million or more cycles of life [7].

4.2. Analytical Optimisation process

The optimization process starts from first entering the physical parameters of spring, material properties, minimum load and valve lift required into the cells of spreadsheet. The equations in the spreadsheet will calculate all the performance parameters required. Then the fallowing strategy is used to find suitable spring data among all other springs. The limiting factors for spring selection are as below.

$$The\ total\ valve\ spring\ contraction \geq (L_f - L_s)$$
$$The\ natural\ frequency\ of\ spring \geq 13 \times cam\ speed$$
$$the\ fatique\ factor\ of\ safety \geq 1.39$$

In addition to "IF & AND functions" of the spread sheet program, the "FILTER" and "UNIQUE" functions are also used for the selection of optimized springs.

4.3. Validation of the analytical results with the finite element method

The analytical results generated using spread sheet program are validated by conducting the simulations of the selected springs in the numerical method software such as Ansys.

4.4. The finite element method using Ansys software

After meshing is successfully performed, the model is applied with needed boundary constraints. ¾ turn at the bottom is fixed, and top one turn is selected for application of load of 760.84 N in negative "Y" direction. Sometime the displacement boundary condition needs to be applied to constrain the movement of spring top turns to freely move in only "Y" direction. Table 3 illustrates the physical dimensions used for the simulations in Ansys software.

Table 3: Physical dimensions of the spring used for the simulation in Ansys

Pitch mm	Turns	Free length mm	Mean Dia mm	Outer wire diameter mm	Inner wire diameter mm
10.8	05	59	33.58	05	2.5

Table 4 shows the settings used in Ansys software for proper simulation.

Table 4: Settings in Ansys for simulation

Element type	Hexahedral	Initial size seed	Assembly
Min Number of elements	15959	Quality/ smoothing	Medium
Max Number of elements	29445	Inflation	Smooth
Adaptive sizing	yes	Growth rate	1.2
Resolution	Default (2)	large deflection	On
Mesh defeaturing	Yes	Weak springs	Off
Transition	Slow	Units	SI System
Span angle centre	Medium		

The below Figure 1,2,3, and 4 show the deflection, equivalent shear stress, Von Mises stress, and natural frequency of the spring under the load of 760.84 N. The deflection is found to be 19.72 mm, shear stress 691.02 MPa, Von Mises stress to be 1247.3 MPa and natural frequency is 633.36 rps.

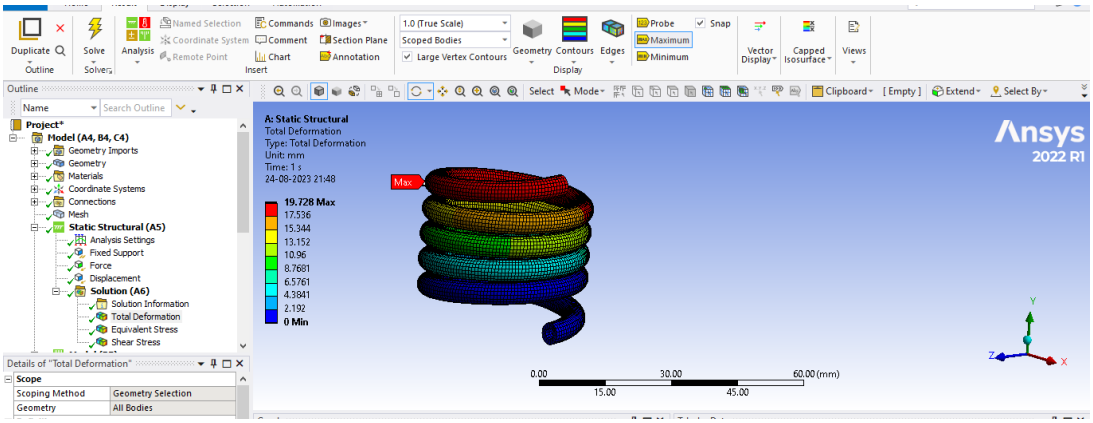

Figure 1: Deflection for the 760.84 N

The maximum Von Mises stress is found from the inner face of the coil by moving the probe tool along the face of inner coils and picking the maximum reading. The value of circular frequency found is 201.71×3.14 =633.36 rps.

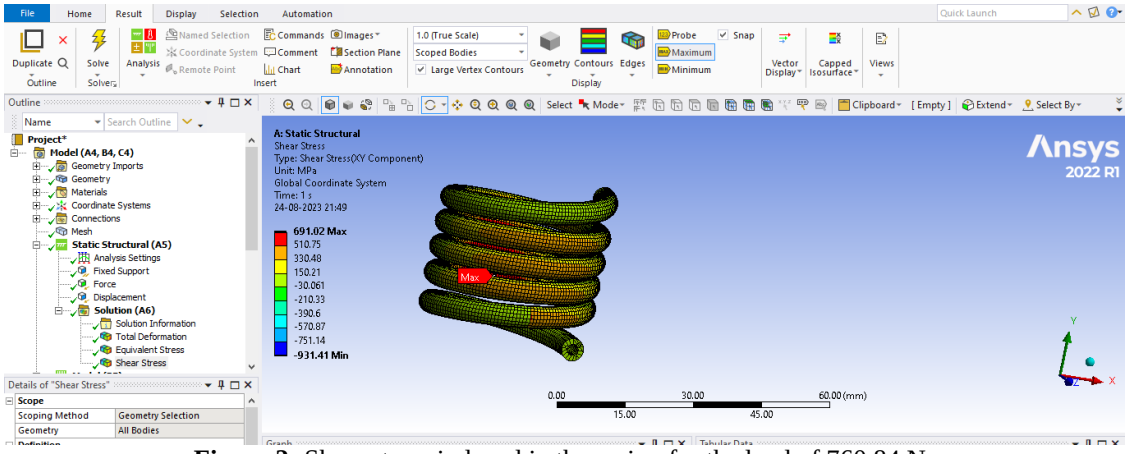

Figure 2: Shear stress induced in the spring for the load of 760.84 N.

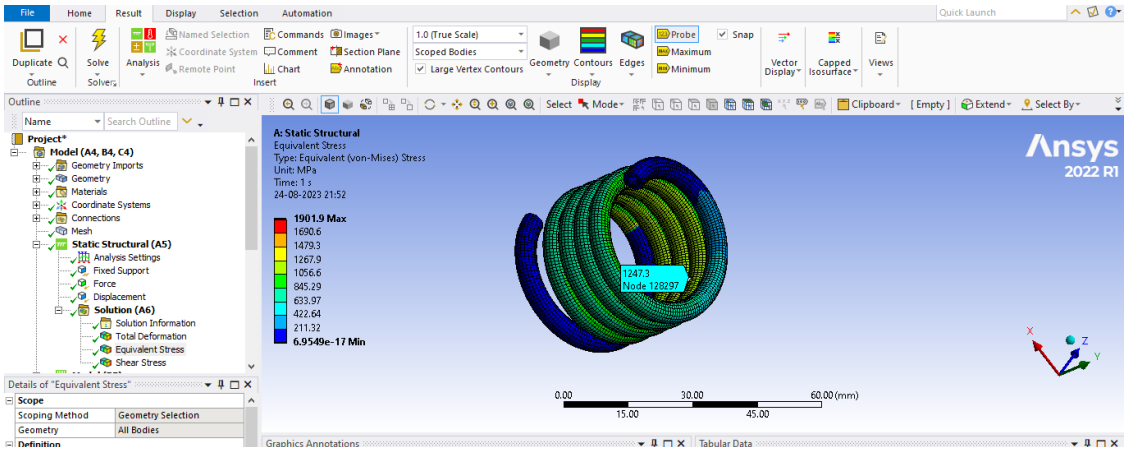

Figure 3: Von-Mise's stress induced in the spring for the load of 760.84N

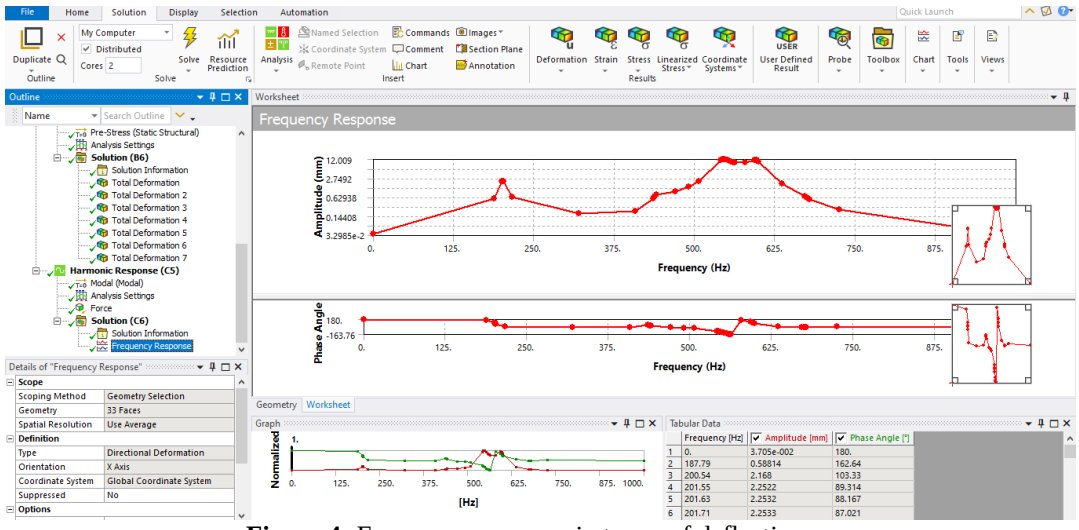

Figure 4: Frequency response in terms of deflection

The table 5 shows the percentage difference between the analytical and FEA results.

Table 5: Comparison of analytical and FEA methods.

Weight, kg		Deflection, mm		Shear stress, MPa		Von Mises stress, MPa		Stiffness, N/mm		Natural Frequency rps	
Analytic	**FEM**	**Analytic**	**FEM**	**Analytic**	**FEM**	**Analytic**	**FEM**	**Analytic**	**FEM**	**Analytic**	**FEM**
0.06	0.06	20.61	19.73	672.1	691	1165	1247	36.92	38.57	633	633.3
Percentage difference between analytical and numerical methods											
0		**4.4**		**-2.81**		**-7**		**-4.4**		**0**	

5. Results and Discussion

Table 6 shows the variation of performance metrics of tubular spring with the bore ratio. The other parameters such as spring index is 6.716 and constant, pitch at 10.8 mm is constant and the load on the spring is also constant at 392 N.

Table 6: Variation of performance metrics with bore ratio of tubular section.

Variation of performance parameter with variation of inner diameter of tubular section for Load 398 N, C=6.716, and Pitch=10.8 mm												
InnDia	**Weight kg**		**Deflection mm**		**Shear stress MPa**		**Von mises stress MPa**		**Stiffness N/mm**		**Natural Frequency rps**	
mm	**Analytic**	**FEA**	**Analytic**	**FEA**	**Analytic**	**FEA**	**Analytic**	**FEA**	**Analytic**	**FEA**	**Analytic**	**FEA**
1.5	0.0739	0.0735	10.01	10.25	327.00	353.05	566.41	610.84	39.13	38.21	406.60	415.20
1.75	0.071	0.0708	10.08	10.37	329.31	354.15	570.38	619.18	38.86	37.78	412.63	418.12
2	0.068	0.0678	10.20	10.47	332.89	361.22	576.85	630.69	38.40	37.42	419.40	423.80
2.5	0.0609	0.0606	10.61	10.94	345.90	372.08	599.20	651.40	36.92	35.82	435.21	436.46
1.9375	0.06845	0.068175	10.23	10.51	333.78	360.13	578.21	628.03	38.33	37.31	418.46	423.40
Percentage difference between analytical and finite element method												
	0.40		-2.74		-7.89		-8.62		2.73		-1.18	

Figure 5 shows the graph of variation of length of contraction with the bore ratio. The contraction is increasing with increase in the bore ratio. The stiffness of the tubular spring will decrease with the bore ratio.

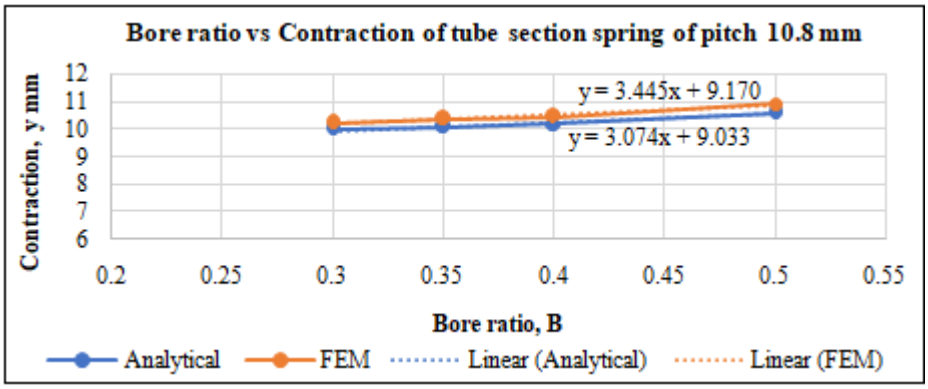

Figure 5: Variation of length of contraction with bore ratio

Figure 6 shows the variation of equivalent shear stress with the bore ratio. The equivalent shear stress is also increasing with respect to bore ratio.

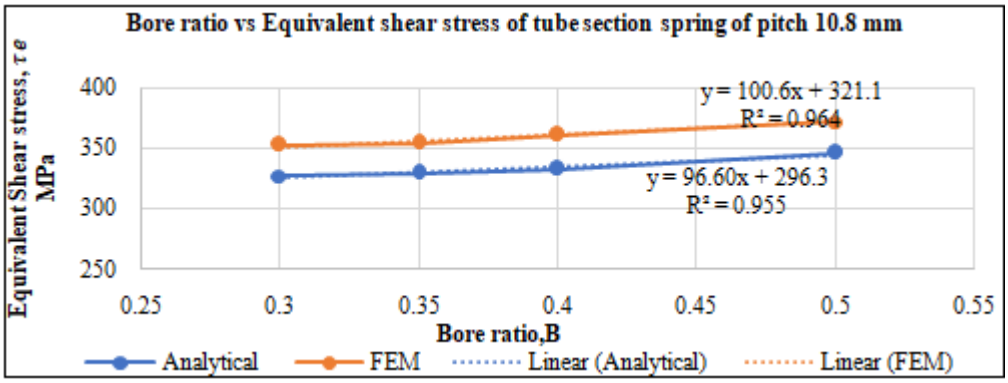

Figure 6: Variation of Equivalent shear stress with bore ratio

Figure 7 shows the effect of bore ratio on the Von Mises stress. The Von Mises stress moderately increases with increase in bore ratio.

Figure 8 shows impact of bore ratio on the rotational natural rate of vibration. The natural rate of vibration also increases a little with the increase in the bore ratio.

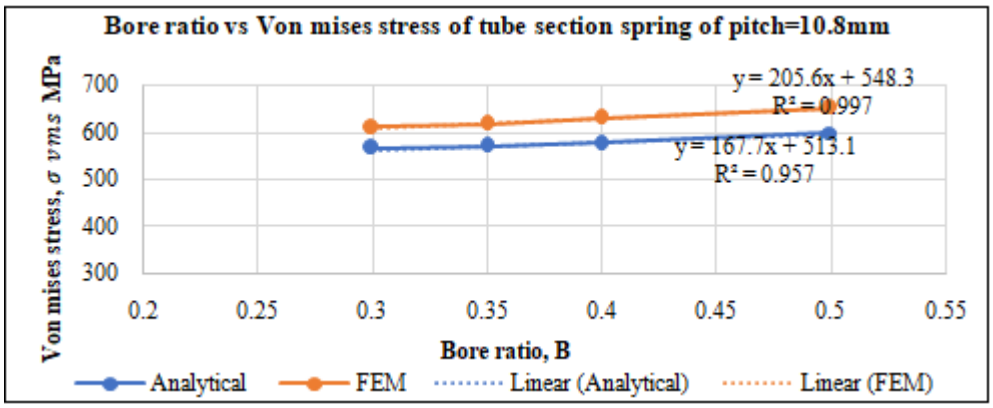

Figure 7: Variation of Von Mises stress with the bore ratio.

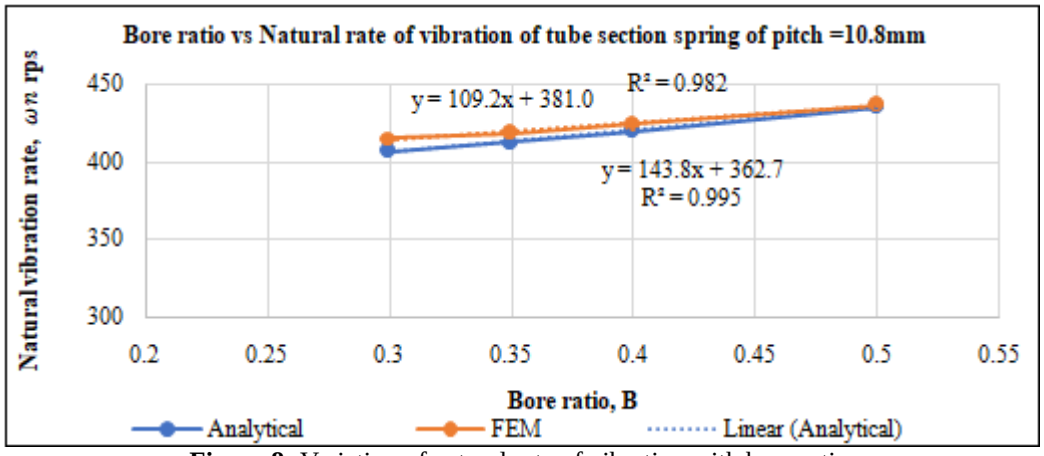

Figure 8: Variation of natural rate of vibration with bore ratio

6. Conclusions

1) The current analytical equations of equivalent shear stress and natural frequency for solid section springs are adjusted for both hollow section springs and to consider the influence of helix angle.
2) The tube section spring's inner diameter and performance metrics including deflection, equivalent shear stress, Von Mises stress, and natural frequency are positively correlated.
3) Stress Vs. Inner Diameter Curve has a steeper slope than the other two. Therefore, compared to natural frequency and deflection, stress varies greater with a unit change in diameter.
4) Using a spreadsheet tool, a simple automated procedure of spring optimization for needed performance metrics is developed.

7. Future Scope

1) Generating analytical equations for other sections of springs such as elliptical, hallow elliptical and ovate.
2) Generating empirical equations to consider the effect of end turn degrees of freedom.
3) Developing a program with graphical user interface to input the data and get the output data.

References

[1] Mosa M, Almuramady N, and Hamzah K. (2020). "Numerical Investigation to Optimizing the Design of Helical Compression Spring by Using Hollow Shaft". Journal of Green Engineering (JGE), 10(7), 3832–3843. http://www.jgenng.com/wp-content/uploads/2020/09/volume10-issue7-36.pdf.

[2] Bert. C. W. (1959). "Helical Springs of Hollow Circular Cross Section". *Journal of Engineering for Industry*. https://doi.org/10.1115/1.4008235 .

[3] Pawar H. B, and Desale D. (2018). "Optimization of Three-Wheeler Front Suspension Coil Spring". Procedia Manufacturing, 20, 428–433. https://doi.org/10.1016/j.promfg. 2018.02.062.

[4] Sagar Singh Kushwaha, Parekh S, & Mangrola M. H. (2021). "Optimization of coil spring by finite element analysis method of automobile suspension system using different materials". 42, 827–831. https://doi.org/10.1016/j.matpr.2020.11.415

[5] Liu H, and Kim D. (2009). "Effects of end coils on the natural frequency of automotive engine valve springs". International Journal of Automotive Technology, 10(4), 413–420. doi:10.1007/s12239-009-0047-8

[6] Taktak M, Khalifa Omheni, Abdessattar Aloui, Fakhreddine Dammak, and Haddar M. (2014). "Dynamic optimization design of a cylindrical helical spring". Applied Acoustics, 77, 178–183. https://doi.org/10.1016/j.apacoust.2013.08.001

[7] Hong Yan Li, Xian Yue Gang, and Chai S. (2011). "Finite Element Analysis of the Valve Spring with Different Engine Speed". *Advanced Materials Research*.

https://doi.org/10.4028/www.scientific.net/amr.382.224

[8] Edwards. G. (1983). "VALVE-SPRING MATERIALS AND DESIGN". Industrial Lubrication and Tribology, 35(2), 44–51. https://doi.org/10.1108/eb053262

[9] Wahl. A. Munzenmaier. (1963). Mechanical springs. Second edition. New York: McGraw-Hill.

[10] Nisbett. K. J, and Budynas. R. G. (2014). *Shigley's Mechanical Engineering design*. McGraw-Hill Education.

[11] Carlson. H. (1978). *Spring Designer's Handbook*. CRC Press.

[12] IGNOU. (2017). *Unit-15 springs*. *https://egyankosh.ac.in/handle/123456789/29500*

[13] Bhandari. V. B. (2020). *Design of machine elements third edition*. McGraw-Hill

[14] *11 things you need to know about Bentley's 6.75-litre V8*. (2020, June 25). Top Gear. https://www.topgear.com/car-news/british/11-things-you-need-know-about-bentleys-675-litre-v8

Author Profile

Jagadish. R. Bagali, M. Tech Final Year student, Machine Design, Mechanical Engineering Department, Basaveshwar Engineering College, Bagalkote

Prof. R. S. Matti, Machine Design, Mechanical Engineering Department, Basaveshwar Engineering College, Bagalkote, 22 Years of Experience

Prof. B. S. Vivekanand, Mechanical Engineering Department, Basaveshwar Engineering College, Bagalkote, 22 Years of Experience